

Article

June–July Temperature Reconstruction of Kashmir Valley from Tree Rings of Himalayan Pindrow Fir

Rayees Malik ^{1,*} and Raman Sukumar ^{1,2} 
¹ Centre for Ecological Sciences, Indian Institute of Science, Bangalore 560012, India; rsuku@iisc.ac.in

² Divecha Centre for Climate Change, Indian Institute of Science, Bangalore 560012, India

* Correspondence: rayeesmalik@iisc.ac.in

Abstract: The Himalaya is one of the major mountain ecosystems that is most likely to be impacted by climate change. The main drawback in understanding climate change in the remote Himalayan ecosystems is the lack of long-term instrumental climate records. Reconstructing past climates from tree-rings offers a useful proxy for adding data to the instrumental climate records. In this study, climatically sensitive tree-rings of Himalayan fir (*Abies pindrow*) were used for reconstruction of mean June–July temperatures of Kashmir valley. Total ring-width chronology was built from 60 tree-ring cores growing near the higher altitudinal limits of the species. The radial growth showed a strong positive response to growing season temperature. The strong response of site chronology to mean June–July temperatures was used for reconstruction purposes. Mean June–July temperatures of Kashmir valley were reconstructed since 1773 from residual site chronology. Though the reconstruction did not show any strong long-term trend, on a centennial-scale, 20th-century summers were the warmest with a mean annual summer temperature of 22.99 °C. Seven of the warmest years and five of the warmest decades were seen in the 20th century. The reconstruction for 1773–2012 showed 23 extreme hot summers above the hot threshold of a 23.47 °C mean temperature and 19 extreme cold years below the cold threshold of a 22.46 °C mean summer temperature. The cold years in the reconstruction did not coincide with known volcanic eruptions. This reconstruction will help in providing a better understanding of regional climate change.

Keywords: climate change; dendroclimatology; total ring-width; Kashmir Himalaya; *Abies pindrow*



Citation: Malik, R.; Sukumar, R. June–July Temperature Reconstruction of Kashmir Valley from Tree Rings of Himalayan Pindrow Fir. *Atmosphere* **2021**, *12*, 410. <https://doi.org/10.3390/atmos12030410>

Academic Editors: Piotr Owczarek, Magdalena Opala-Owczarek and Feng Chen

Received: 10 February 2021

Accepted: 18 March 2021

Published: 23 March 2021

Publisher's Note: MDPI stays neutral with regard to jurisdictional claims in published maps and institutional affiliations.



Copyright: © 2021 by the authors. Licensee MDPI, Basel, Switzerland. This article is an open access article distributed under the terms and conditions of the Creative Commons Attribution (CC BY) license (<https://creativecommons.org/licenses/by/4.0/>).

1. Introduction

The ongoing climate change accompanied by an increase in temperature, changes in precipitation, shrinking of glaciers, and decreasing snow cover, has a significant impact on ecosystem dynamics as well as on social communities [1,2]. High mountains around the globe are some of the most vulnerable regions to climate change. The Himalayas are warming faster than the global average [3]. The warming of the Himalayas will have impacts on water resources, species distribution, ecosystem dynamics, agricultural systems, and the well-being of a large proportion of people [4]. There are many studies which have shown that temperature is increasing in the Himalayas [3,5]. The temperature in the northwestern Himalayas has risen by 1.6 °C in the last century, with the warming being more noticeable during the winter months. On the other hand, some studies show an increasing trend in annual precipitation [3] while an overall decreasing trend was found in another study [6].

Climatic data over several decades or a century are needed to understand the climatic fluctuations at a regional scale. The problem with remote mountainous areas is the lack of long instrumental climatic data. To extend the short instrumental data, many proxies such as ice cores, peat bogs, pollen, and tree rings are commonly used. Trees record the environmental information in their annual growth-rings [7,8]. Climate is considered to be one of the most important factors limiting the growth of trees, particularly near

the ecological boundaries of a species [9]. The year to year variation in the tree ring parameters reflects the change in the limiting climatic factor. The main advantage of the climatic data reconstructed from tree-rings is that it is annually resolved, well-calibrated, and verified [10].

The trees from the Himalayas have shown great dendroclimatic potential owing to their great age and high climatic sensitivity [11–13]. Over the past three decades, many regional climate reconstructions have been done using Himalayan trees [14–16]. In the Kashmir valley, tree-ring studies were started by the Tree-ring Laboratory, University of Arizona, USA, on ring-width and wood densities of *Abies pindrow* and *Picea smithiana* [17]. The data were reanalyzed and published in 1992 in a book titled “Climate since AD 1500” [18]. Later, in 2001 an improved reconstruction of summer temperatures at Srinagar, Jammu, and Kashmir since 1660 AD was done based on total ring-width and maximum latewood density of *A. pindrow* [19]. Stable isotopes (δD , $\delta^{13}C$ and $\delta^{18}O$) of tree-ring cellulose from *A. pindrow* collected from Gulmarg, Jammu, and Kashmir showed sensitivity to growing season precipitation and mean maximum temperatures [20,21]. Since then, other tree-ring studies have been done in the Kashmir valley during the past two decades [22–24]. Summer precipitation at Srinagar was reconstructed since the late-18th century from *A. pindrow* and *P. smithiana* ring-width chronologies [23]. The tree-ring chronologies of *A. pindrow* and *P. smithiana* were shown to significantly respond to the Palmer drought severity index (PDSI) and the relationship was utilized to reconstruct the PDSI of Srinagar from 1820–1981 [25]. Recently, the precipitation of Lidder Valley in Kashmir was reconstructed since 1723 from *Cedrus deodara* chronologies [24]. All these chronologies except for the *C. deodara* chronology were composed of a small number (4–25) of tree cores [24]. The objective of the present study was to develop a robust summer temperature reconstruction of the Kashmir valley for a better understanding of regional climate fluctuations.

2. Materials and Methods

2.1. Study Area

The valley of Kashmir lies between 33°20' to 34°54' N latitudes and 73°55'–75°35' E longitudes covering an area of approximately 15,948 km² and is surrounded by Karakoram range in the north, Pir-panjal range in the south and west, Zaskar range in the east, and Siwalik hills towards the south.

This study was carried out in Hirpora Wildlife Sanctuary (HWS) in district Shopian, Jammu and Kashmir (33,066' N, 74,068' E) (Figure 1). The HWS lies in the Pir-panjal range of northwestern Himalaya approximately 70 km south-west of Srinagar city covering an area of approximately 341 km². The HWS forest type is a mixed coniferous forest with sub-alpine and alpine pastures at the higher altitudes. The most abundant conifer species growing in the HWS is *Abies pindrow* which is the dominant tree species on the northern aspects of the sanctuary. The other conifer species include *Picea smithiana* and *Pinus wallichiana*.

2.2. Climate of the Study Area

Hirpora Wildlife Sanctuary has a sub-humid temperate climate. There is no weather station in the HWS, so climate data of Srinagar meteorological station was used for this study (Figure 2). The Srinagar station is the only station with more than 100 years of climate data in the Kashmir valley. For this study, station climate data for the period 1960–2012 was used. As recorded from the meteorological station, the mean annual temperature of Srinagar was 13.9 °C and mean annual precipitation was approximately 664 mm during the analyzed period (Figure 2). The maximum temperature of the warmest month (July) was 29.9 °C and the minimum temperature of the coldest month (January) was −2.0 °C. Temperature goes to sub-zero in winter months. March–May is the wet season in Kashmir while precipitation falls in the form of snow during the winter months of December–February. The valley is a monsoon shadow zone because of the mighty Himalayan range, with the weather mainly affected by the Westerlies [26].

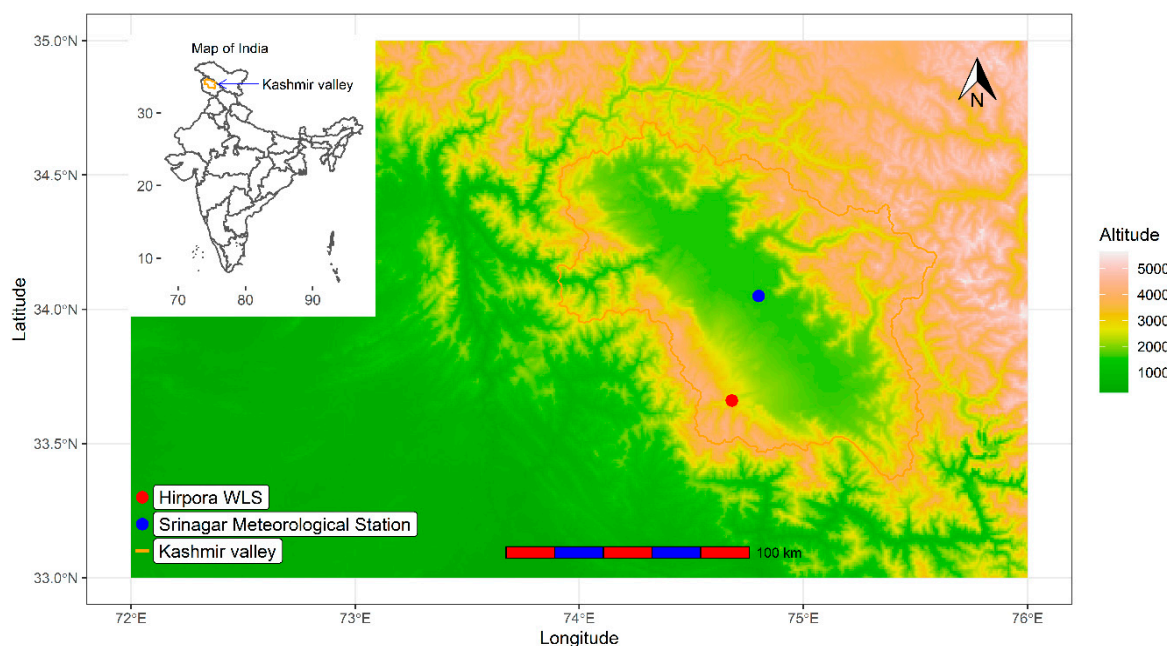


Figure 1. Map of the sampling site and meteorological station in northwestern Himalaya.

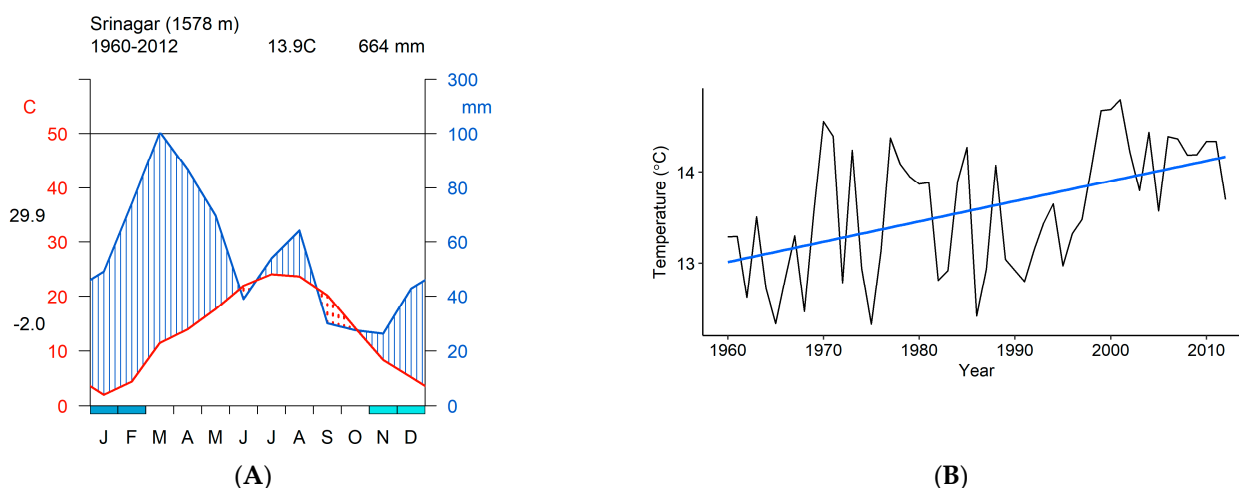


Figure 2. (A) Monthly climate diagram of Srinagar based on instrumental data from Srinagar meteorological station. (B) The long-term mean annual temperature of Srinagar (1960–2012).

The mean annual temperature in Himalaya has shown an increasing trend of $0.06\text{--}0.1\text{ }^{\circ}\text{C yr}^{-1}$ since the mid-1970s, which is higher than the global average [3,27,28]. More specifically, the mean annual temperature has increased by $1.6\text{ }^{\circ}\text{C}$ during the last century in northwestern Himalaya, with the maximum temperature showing a more rapid increase. Winter temperatures have shown a more noticeable increase as compared to summer temperatures in the last century [29].

2.3. Chronology Development and Statistical Analysis

A total of 60 increment cores from 44 old and healthy trees of *A. pindrow* were collected during 2014–2016, usually towards the end of the growing season near the higher altitudinal limits (2950–3250 m a.s.l.). The cores were stored in drinking straws and transported to the laboratory for further analysis. In the laboratory, the cores were glued to wooden holders and sequentially sanded using progressively finer grit sandpapers (80–3000 grit). The sanded cores were scanned in a high-resolution Espion Perfection V700 Photo scanner[®] at 2400 dpi to make ring boundaries clearly visible. The scanned images were saved in

the JPEG format, which is compatible with CooRecorder/CDendro software [30]. The ring-width measurements were done in CooRecorder/CDendro software package. Measurements were first visually cross-dated and cross-checked with the computer program COFECHA [31] and dplR [32] to ensure that each ring is assigned to its correct year of formation. COFECHA is a statistical tool in dendrochronology used for crossdating purposes [33]. The raw site chronology was built by taking the robust mean of all the series. Various descriptive statistics such as the average mean sensitivity, series inter-correlation, and expressed population signal (EPS) were computed (Table 1). The sample size fulfilling the required threshold value of EPS 0.85 is expected to capture the theoretical population signal in a site and, hence, its usefulness for dendroclimatological analysis [34].

Table 1. Descriptive statistics of site chronology.

Time Span	No. of Trees	No. of Cores	Mean Sensitivity	Series Inter-Correlation	1st Order Auto-Correlation	EPS > 0.85
1578–2012	44	60	0.18	0.47	0.54	1773–2012

The raw ring-width series were standardized to convert them into dimensionless indices using the dplR package [35] in the R statistical program [36]. To remove the non-climatic age-related growth trends and other individualistic trends, the raw ring-width series were detrended using a cubic spline curve of 32 years and the ratios were calculated. The main criteria for detrending were to minimize the non-climatic low-frequency trend and maximize the high-frequency trend. The detrended series were averaged by computing bi-weight robust mean to make a standard site chronology [37].

The standardized site chronology showed high first-order auto-correlation values because of the impact of the previous year's weather on current year's tree growth. This persistence in the standard chronology was removed by autoregressive modeling and the resulting residual series were averaged by computing the bi-weight robust mean to make a residual site chronology [37] (Figure 3).

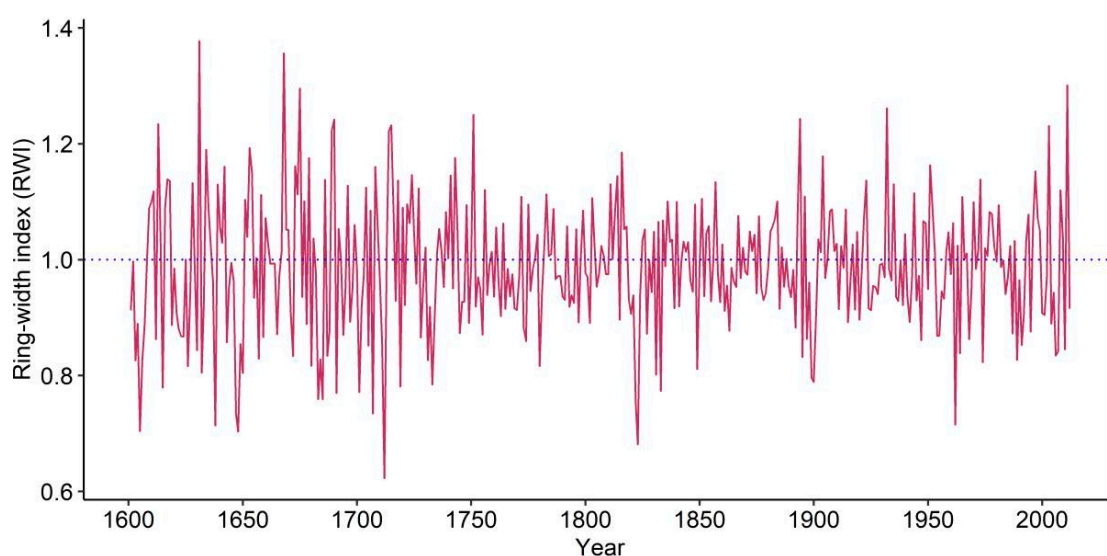


Figure 3. Residual site chronology of *A. pindrow* from high elevation limits of Hirpora Wildlife Sanctuary.

Static bootstrapped correlations were calculated between site chronology and single growing-season months [38,39] and biologically relevant monthly combinations in R statistical software [36].

A linear regression was computed between the tree-ring width series and mean June–July temperature for the period 1960–2012. The skill of the climate-reconstruction model

was assessed using calibration and verification statistics (Figure 4). Verification statistical parameters included the reduction of error (RE), coefficient of efficiency (CE), and root mean squared error (RMSE) [40].

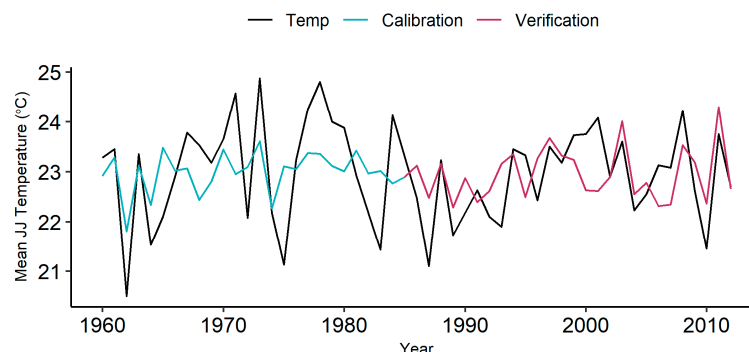


Figure 4. Comparison of the actual and reconstructed mean June–July temperature of Srinagar for the common period 1960–2012.

Wavelet analysis was performed to characterize the variability of final June–July (JJ) temperature reconstruction in temporal and spectral domain [41]. This procedure helps to check for potential periodicities in climate reconstruction.

3. Result

Figure 5 below shows the correlations between residual site chronology and monthly temperature from growing season April (a) to August (A). The strong positive response of radial growth to monthly temperature with statistically significant positive correlations with June ($R = 0.35$; $p < 0.01$), July ($R = 0.45$; $p < 0.01$), April–July ($R = 0.29$; $p < 0.05$), May–July ($R = 0.38$; $p < 0.01$), May–August ($R = 0.32$; $p < 0.05$), June–July ($R = 0.48$; $p < 0.01$), June–August ($R = 0.38$; $p < 0.01$), and July–August ($R = 0.30$; $p < 0.05$) temperatures were seen. Based on the monthly combinations, the highest correlation ($R = 0.48$, $p < 0.01$) was found between tree-ring width series and mean June–July temperature. The strong relationship between mean June–July temperature and site chronology was used for past climate reconstruction purposes.

Based on the above correlation analysis results, a linear regression model (Figure 6) was developed between the ring-width series and the mean June–July temperature as follows:

$$Y = 19 + 4.3X, \quad (1)$$

where Y is the mean June–July temperature and X is the ring-width index.

During the calibration period 1960–1985, the model accounts for 26% of the total variance of the instrumental data. The results of reduction of error (RE), coefficient of efficiency (CE) and root mean squared error (RMSE) during the verification period are shown in Table 2. Based on good reconstruction skills of the model in the verification period, the reconstruction of mean June–July temperature was done since 1773 ($EPS > 0.85$).

The 10 coldest years in reconstruction (Figure 7), in increasing order, were 1823, 1962, 1822, 1833, 1900, 1899, 1831, 1849, 1780, and 1974 while the 10 warmest years, in decreasing order, were 2011, 1932, 1894, 2003, 1816, 1904, 1951, 1997, 1814, and 1973, with 1823 being the coldest summer and 2011 the warmest with mean JJ temperature of 21.66 °C and 24.30 °C, respectively. Seven of the 10 warmest years were seen after the beginning of the 20th century while seven of the coldest years were seen prior to the 20th century. On a decadal scale, the 10 warmest decades were 1810, 1900, 1970, 1930, 1850, 1880, 1780, 1990, 1950, and 1870, with 1810 being the warmest decade with a decadal mean temperature of 23.2 °C. The 10 coldest decades in the reconstruction were 1820, 1890, 2000, 1960, 1860, 1980, 1910, 1940, 1790, and 1840 with 1820 being the coldest decade with a decadal mean temperature of 22.7 °C. Nevertheless, the 20th century is clearly the warmest century with

a mean annual JJ temperature of 22.99 °C, including 5 of the 10 warmest decades. The coldest years in the chronology did not correlate with any known volcanic eruption because known eruptions occurred far away from the study site.

The extreme hot and cold summers were recorded based on the lower and upper threshold as the 10th and 90th percentile, respectively. The reconstruction from 1773–2012 showed 23 extreme hot summers above the hot threshold of 23.47 °C mean temperature and 19 extreme cold years below the cold threshold of 22.46 °C mean summer temperature. All the extreme hot years were single-year events while as three of the cold events were of 2-year duration (1822–1823, 1899–1900 and 1954–1955). The longest warm/cold periods of three or more years with a temperature greater/less than the instrumental mean temperature are provided in Table 3. The longest warm period of seven years occurred during the latter part of 20th century (1975–1981) while the longest cold periods of six years occurred during the early 19th century (1819–1824), mid-19th century (1861–1866), and early 20th century (1924–1929).

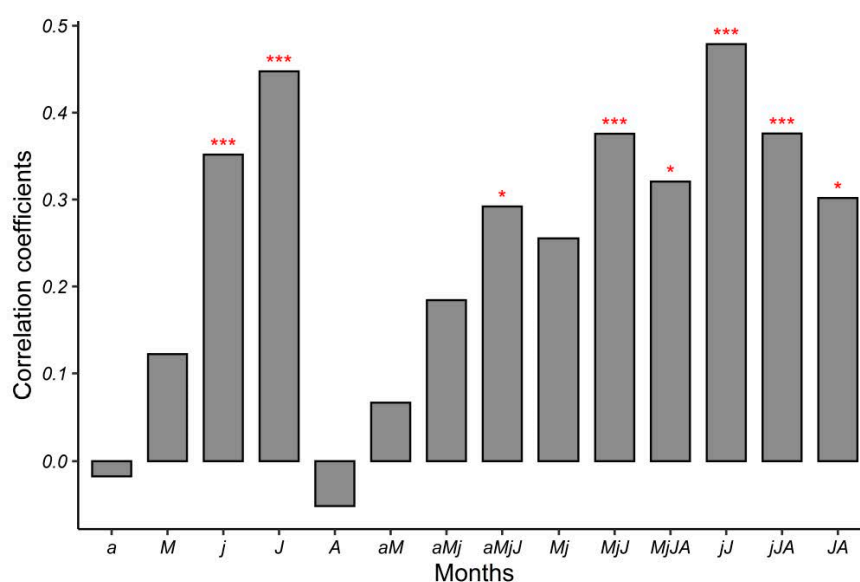


Figure 5. Correlation coefficients between radial growth of *A. pindrow* and monthly as well as multi-month combination temperature from current April to August (The horizontal tick labels show the current year months and monthly combinations from April–August and the asterisk marks * & *** above bars show statistical significance at $p < 0.05$ and $p < 0.01$, respectively).

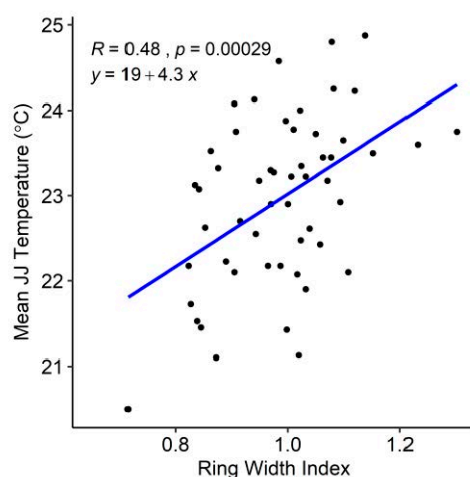


Figure 6. Linear regression between mean June–July temperature and ring width indices.

Table 2. The calibration-verification statistics of mean June–July temperature reconstruction.

Whole Period (1960–2012)		Calibration Period (1960–1985)		Verification Period (1986–2012)		
R	p-Value	R	p-Value	RE	CE	RMSE
0.48	<0.001	0.51	<0.001	0.29	0.26	0.98

RE = Reduction of error; CE = Coefficient of efficiency; RMSE = Root mean squared error.

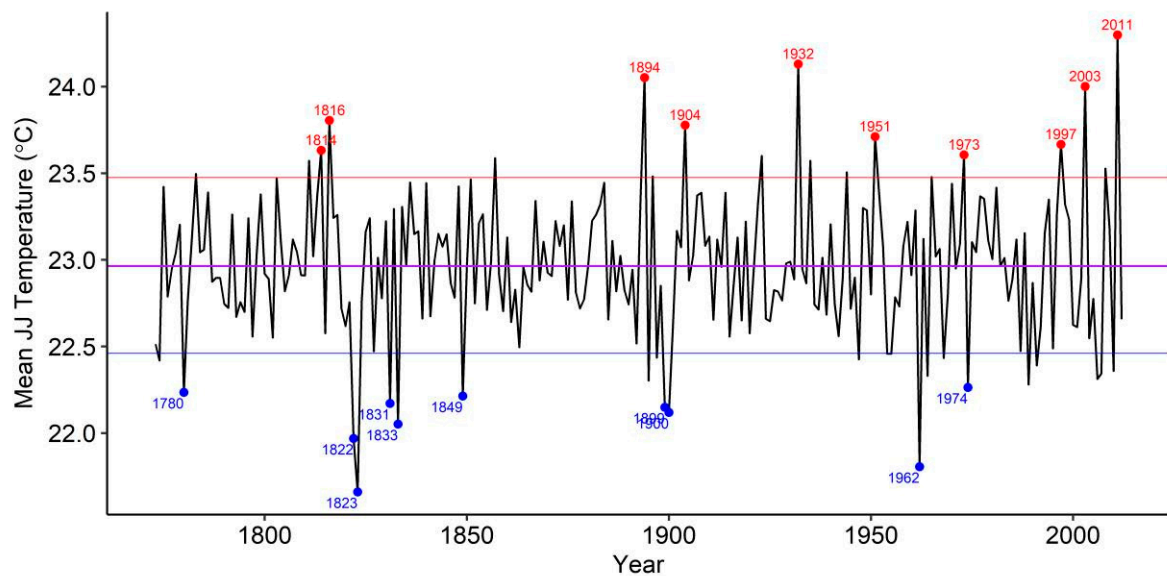


Figure 7. Reconstructed mean June–July temperatures of Srinagar during 1773–2012. The horizontal purple line is the mean June–July temperature of the instrumental data whereas the blue and red horizontal lines indicate 10th and 90th percentiles, respectively. The red and blue solid circles/text indicate the top 10 warm and cool years, respectively.

Table 3. Warm and cold periods from the reconstruction of mean June–July temperature of Srinagar, Jammu, and Kashmir, India during 1773–2012.

Warm Periods (Duration in Years)	Cold Periods (Duration in Years)
1782–1786 (5)	1787–1791 (5)
1811–1814 (4)	1793–1795 (3)
1816–1818 (3)	1800–1802 (3)
1836–1838 (3)	1819–1824 (6)
1842–1845 (4)	1861–1866 (6)
1872–1874 (3)	1877–1880 (4)
1881–1884 (4)	1889–1892 (4)
1902–1904 (3)	1897–1901 (5)
1906–1910 (5)	1924–1929 (6)
1951–1953 (3)	1941–1943 (3)
1965–1967 (3)	1945–1947 (3)
1975–1981 (7)	1954–1957 (4)
1996–1999 (4)	1989–1992 (4)
	2000–2002 (3)
	2004–2007 (4)

The variability of reconstructed JJ temperature of Srinagar was further investigated in the spectral domain (Figure 8). Wavelet analysis of JJ temperature reconstruction revealed significant spectral peaks between 2–14 year cycles; however, the occurrence of these cycles is temporally unstable.

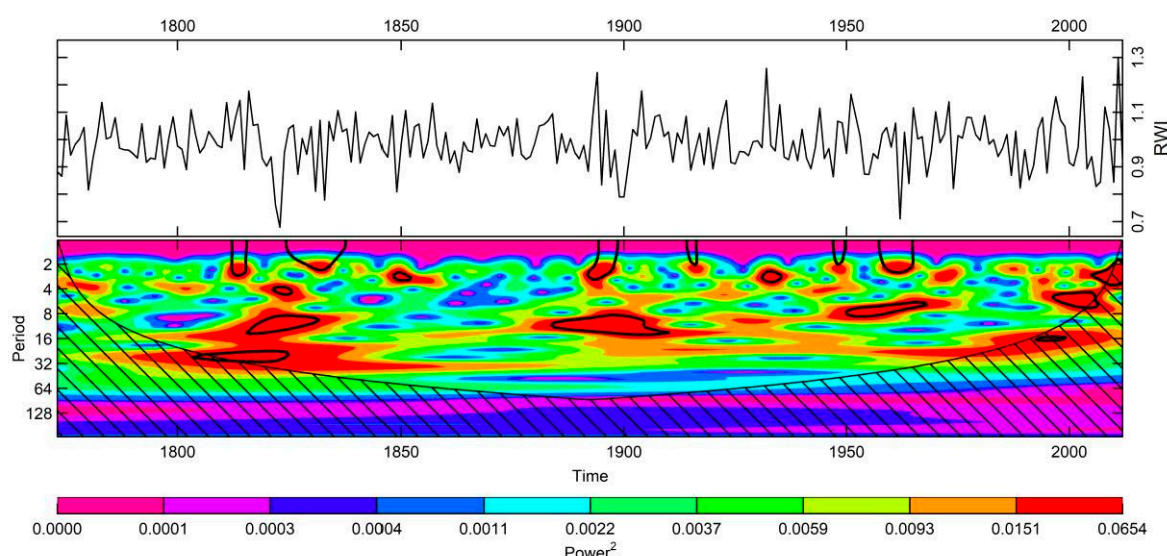


Figure 8. Wavelet power spectrum of *A. pindrow* tree-ring index.

4. Discussion

This summer temperature reconstruction is only the third temperature reconstruction from Kashmir valley after Hughes (1992; 2001). The earlier two reconstructions were based on a lower number of samples. The overall radial growth patterns of *A. pindrow* in the Hirpora residual chronology were similar to those found in the residual site chronologies of Hughes (Figure 9). Of various sites investigated by Hughes (1992; 2001), the radial growth recorded by us at Hirpora was more related with that of Khilanmarg ($R = 0.55$, $p < 0.01$) which is situated in close proximity to Hirpora in the Pir-Panjal range of the Himalayas.

The positive response of tree growth to the temperature at tree-line site is more of a general phenomenon [42]. Radial growth generally reflects variations in growing season temperature at high elevations in mountain regions [43]. Higher temperatures could increase the rate of photosynthesis and thus enhancing radial growth [44].

High temperatures in the growing season reduce radial growth at lower altitudes, whereas high temperatures during summer promote radial growth at higher altitudes. Most of the xylogenesis (wood formation) process in Himalayan fir in this region occurs during April–September [39]. Also, the daily rate of tracheid formation is highest near the summer solstice [38], thereby revealing the importance of warm summers for radial growth in mountain regions. The increasing summer temperatures result in the lengthening of growing season duration and, hence, more radial growth at higher altitudinal limits of the species [39]. Generally, precipitation and soil moisture increase with increasing altitude, whereas air temperature decreases with increasing altitude, suggesting that radial growth in *A. pindrow* at upper limits was limited more by low temperature than by precipitation [10]. The growth-climate relationship studies on high-elevation conifers in southwestern China also showed the positive response of the radial growth in fir to warm summer temperatures [45]. Overall, these results are in agreement with other studies showing that radial growth responds positively to growing season precipitation at lower altitudes, whereas radial growth responds positively to growing season temperatures at higher altitudes [42,46]. The positive response of radial growth to growing season temperatures and the linear increase of growing season duration with increasing temperature as revealed by the cambial phenology study in this species [38] suggest the positive impact of ongoing climate warming on radial growth in this conifer species.

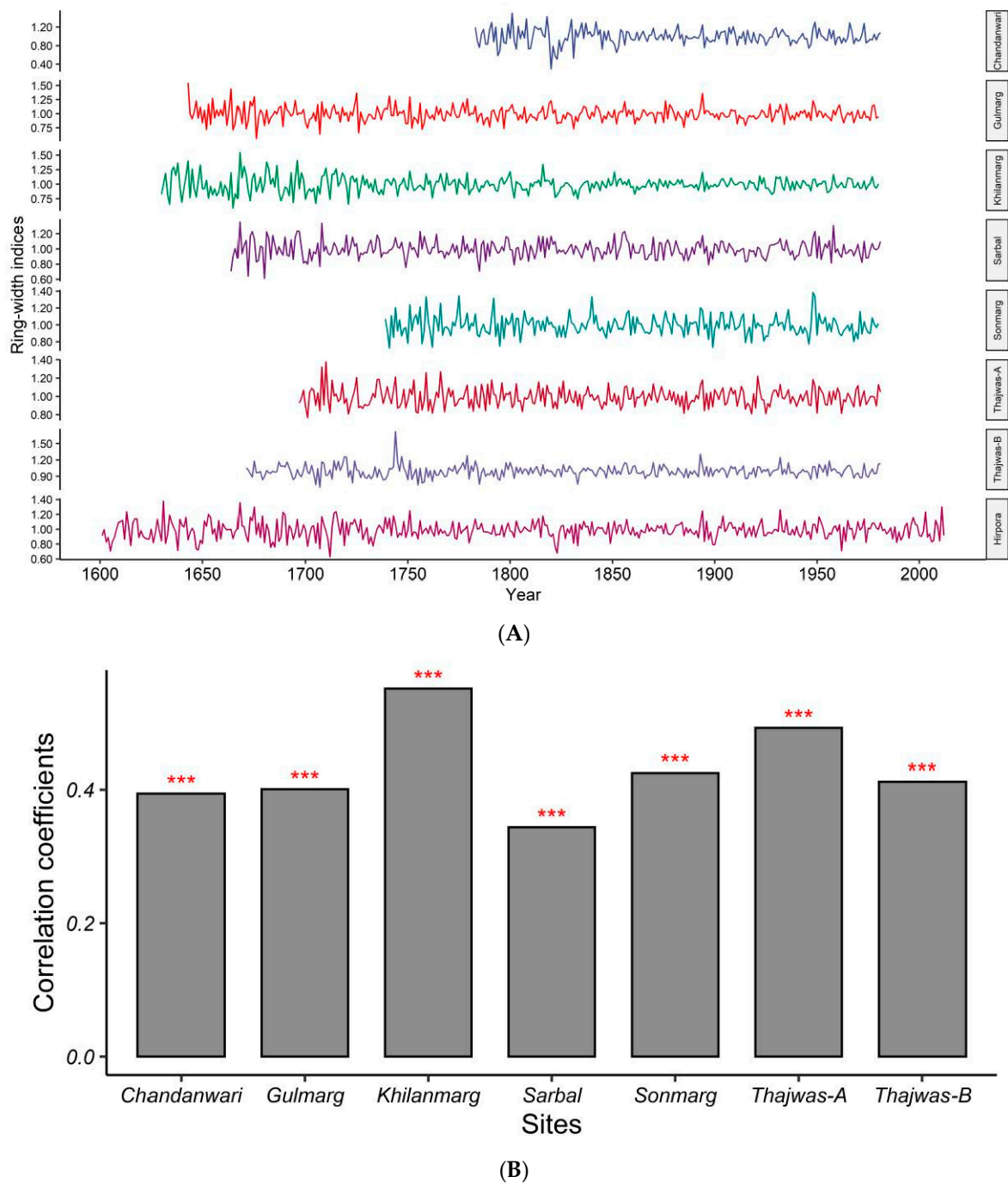


Figure 9. (A) Residual site chronologies of Hirpora and various sites sampled by M K Hughes [17,18]. (B) Correlation plot showing correlation coefficients between Hirpora and other residual site chronologies (The asterisk marks *** above bars show statistical significance at $p < 0.01$).

This reconstruction captured some of the annual and decadal trends, but there was no strong evidence of any long-term trend. There was no clear relationship between known volcanic eruptions and the reconstructed cool summers, as was also reported in the earlier reconstruction [19]. The temperature reconstruction shows that the 19th century was the coldest period, while there are increasing summer temperatures seen in the later parts of the 20th century. Overall, five of the warmest decades were recorded in the 20th century while four of the coldest decades were recorded in the 19th century. The occurrence of seven of the top 10 warmest years and 05 of the top 10 warmest decades in the 20th century further corroborates the century being the warmest one. Wavelet analysis

indicates that the summer temperature cycles have not remained constant during the last two centuries. There are also no significant multi-decadal cycles seen in the summer temperature reconstruction.

This reconstruction added 128 years during 1773–1900 to the instrumental climate data of Srinagar, Jammu, and Kashmir. This will help in understanding the variations in northwestern Himalayan climate on a long-term scale.

This study highlights the importance of the Himalayan conifers in recording the variability in climatic factors. There is, however, a need to develop reconstructions based on samples from more sites across the northwestern Himalayas to better understand the climate variability of and assess the impacts of climate change on the region.

5. Conclusions

In this study, the past climate reconstruction potential of *A. pindrow* was studied and the mean June–July temperature of Kashmir valley was reconstructed since 1773. The Himalayan pindrow fir showed a strong positive response to monthly temperatures in the analyzed time-period. The strong positive response of radial growth to mean June–July temperatures during 1960–2012 was used for past climate reconstruction. The reconstruction added 128 more years to the instrumental climate data of Kashmir valley. The reconstruction revealed some annual and decadal trends but did not show any strong long-term trend. This study will help in creating a better understanding of regional climate change.

Author Contributions: R.M. collected data, analyzed data, wrote manuscript while R.S. acquired funding, approvals, supervision and editing/reviewing of the manuscript. All authors have read and agreed to the published version of the manuscript.

Funding: This research received no external funding.

Institutional Review Board Statement: Not applicable.

Informed Consent Statement: Not applicable.

Data Availability Statement: Hughes, M.K. tree ring datasets were downloaded from International Tree-Ring Data Bank website: <https://www.ncdc.noaa.gov/data-access/paleoclimatology-data/datasets/tree-ring> (accessed on 17 March 2021).

Acknowledgments: We thank Divecha Centre for Climate Change, IISc Bangalore for their funding support for this project. Also, thanks to Jammu and Kashmir Wildlife Department for giving permission to carry out this work in Hirpora Wildlife Sanctuary, J&K. RS was a JC Bose National Fellow during the tenure of this study.

Conflicts of Interest: The authors declare no conflict of interest.

Submission Declaration and Verification: This work has not been published previously and is not under consideration for publication elsewhere. Consent to submit has been received explicitly from all co-authors, as well as from the responsible authorities, before submission of the manuscript. Authors whose names appear on the submission have contributed sufficiently to the scientific work and therefore share collective responsibility and accountability for the results.

References

1. Shepherd, A.; Wingham, D. Recent Sea-Level Contributions of the Antarctic and Greenland Ice Sheets. *Science* **2007**, *315*, 1529–1532. [CrossRef] [PubMed]
2. Webster, P.J. Changes in Tropical Cyclone Number, Duration, and Intensity in a Warming Environment. *Science* **2005**, *309*, 1844–1846. [CrossRef] [PubMed]
3. Shrestha, U.B.; Gautam, S.; Bawa, K.S. Widespread Climate Change in the Himalayas and Associated Changes in Local Ecosystems. *PLoS ONE* **2012**, *7*, e36741. [CrossRef]
4. Immerzeel, W.W.; van Beek, L.P.H.; Bierkens, M.F.P. Climate Change Will Affect the Asian Water Towers. *Scienc.* **2010**, *328*, 1382–1385. [CrossRef] [PubMed]

5. Bhutiyani, M.R. Climate Change in the Northwestern Himalayas. In *Dynamics of Climate Change and Water Resources of Northwestern Himalaya*; Society of Earth Scientists Series; Joshi, R., Kumar, K., Palni, L., Eds.; Springer: Cham, Switzerland, 2015; pp. 85–96. ISBN 978-3-319-13742-1. [\[CrossRef\]](#)
6. Bhutiyani, M.R.; Kale, V.S.; Pawar, N.J. Climate change and the precipitation variations in the northwestern Himalaya: 1866–2006. *Int. J. Climatol.* **2010**, *30*, 535–548. [\[CrossRef\]](#)
7. Cook, E.R.; Anchukaitis, K.J.; Buckley, B.M.; D’Arrigo, R.D.; Jacoby, G.C.; Wright, W.E. Asian Monsoon Failure and Megadrought During the Last Millennium. *Science* **2010**, *328*, 486–489. [\[CrossRef\]](#)
8. Wilson, R.; Miles, D.; Loader, N.J.; Melvin, T.; Cunningham, L.; Cooper, R.; Briffa, K. A millennial long March–July precipitation reconstruction for southern-central England. *Clim. Dyn.* **2013**, *40*, 997–1017. [\[CrossRef\]](#)
9. Fritts, H.C. *Tree Rings and Climate*; Elsevier: Cambridge, MA, USA, 1976.
10. Bradley, R.S.; Fritts, H.C. Tree Rings and Climate. *Arct. Alp. Res.* **1978**, *10*, 144. [\[CrossRef\]](#)
11. Bhattacharyya, A.; LaMarche, V.C., Jr.; Telewski, F.W.; Lamarche, V.; Telewski, F.W.; LaMarche, V.C., Jr.; Telewski, F.W. Dendrochronological Reconnaissance of the Conifers of Northwest India. *Tree Ring Bull.* **1988**, *48*, 21–30.
12. Borgaonkar, H.P.; Sikder, A.B.; Ram, S. High altitude forest sensitivity to the recent warming: A tree-ring analysis of conifers from Western Himalaya, India. *Quat. Int.* **2011**, *236*, 158–166. [\[CrossRef\]](#)
13. Gaire, N.P.; Bhujju, D.R.; Koirala, M.; Shah, S.K.; Carrer, M.; Timilsena, R. Tree-ring based spring precipitation reconstruction in western Nepal Himalaya since AD 1840. *Dendrochronologia* **2017**, *42*, 21–30. [\[CrossRef\]](#)
14. Chaudhary, V.; Bhattacharyya, A.; Guiot, J.; Shah, S.K.; Srivastava, S.K.; Edouard, J.-L.; Thomas, A. Reconstruction of August–September temperature in North-Western Himalaya since AD 1773, based on tree-ring data of *Pinus Wallichiana* and *Abies Pindrow*. In *Holocene: Perspectives, Environmental Dynamics and Impact Events*; Nova Science Publishers: New York, NY, USA, 2013; pp. 145–156.
15. Treydte, K.S.; Schleser, G.H.; Helle, G.; Frank, D.C.; Winiger, M.; Haug, G.H.; Esper, J. The twentieth century was the wettest period in northern Pakistan over the past millennium. *Nature* **2006**, *440*, 1179–1182. [\[CrossRef\]](#) [\[PubMed\]](#)
16. Singh, J.; Yadav, R.R.; Wilmking, M. A 694-year tree-ring based rainfall reconstruction from Himachal Pradesh, India. *Clim. Dyn.* **2009**, *33*, 1149–1158. [\[CrossRef\]](#)
17. Hughes, M.K.; Davies, A. Dendroclimatology in Kashmir Using Tree-Ring Widths and Densities in Subalpine Conifers. In *Methods of Dendrochronology: East-West Approaches*; Kairiukstis, L.A., Bednars, Z., Feliksik, E., Eds.; Polish Academy of Sciences: Warsaw, Poland, 1987; pp. 163–176.
18. Hughes, M.K. Dendroclimatic evidence from the western Himalaya. In *Climate Since AD 1500*; Bradley, R.S., Jones, P.D., Eds.; Routledge Press: London, UK, 1992; pp. 415–431.
19. Hughes, M.K. An improved reconstruction of summer temperature at Srinagar, Kashmir since 1660 AD, based on tree-ring width and maximum latewood density of *Abies pindrow* [Royle] Spach. *Palaeobotanist* **2001**, *50*, 13–19.
20. Ramesh, R.; Bhattacharya, S.K.; Gopalan, K. Climatic correlations in the stable isotope records of silver fir (*Abies pindrow*) trees from Kashmir, India. *Earth Planet. Sci. Lett.* **1986**, *79*, 66–74. [\[CrossRef\]](#)
21. Ramesh, R.; Bhattacharya, S.K.; Gopalan, K. Dendroclimatological implications of isotope coherence in trees from Kashmir Valley, India. *Nature* **1985**, *317*, 802–804. [\[CrossRef\]](#)
22. Ram, S.; Borgaonkar, H.P. Climatic response of various tree ring parameters of fir (*Abies pindrow*) from Chandanwadi in Jammu and Kashmir, western Himalaya, India. *Curr. Sci.* **2014**, *106*, 1568–1576.
23. Borgaonkar, H.P.; Pant, G.B.; Rupa Kumar, K. Dendroclimatic reconstruction of summer precipitation at Srinagar, Kashmir, India, since the late-eighteenth century. *Holocene* **1994**, *4*, 299–306. [\[CrossRef\]](#)
24. Shah, S.K.; Pandey, U.; Mehrotra, N. Precipitation reconstruction for the Lidder Valley, Kashmir Himalaya using tree-rings of *Cedrus deodara*. *Int. J. Climatol.* **2018**, *38*, e758–e773. [\[CrossRef\]](#)
25. Ram, S. Tree growth–climate relationships of conifer trees and reconstruction of summer season Palmer Drought Severity Index (PDSI) at Pahalgam in Srinagar, India. *Quat. Int.* **2012**, *254*, 152–158. [\[CrossRef\]](#)
26. Dimri, A.P.; Niyogi, D.; Barros, A.P.; Ridley, J.; Mohanty, U.C.; Yasunari, T.; Sikka, D.R. Western Disturbances: A review. *Rev. Geophys.* **2015**, *53*, 225–246. [\[CrossRef\]](#)
27. Pandey, S.; Carrer, M.; Castagneri, D.; Petit, G. Xylem anatomical responses to climate variability in Himalayan birch trees at one of the world’s highest forest limit. *Perspect. Plant Ecol. Evol. Syst.* **2018**, *33*, 34–41. [\[CrossRef\]](#)
28. Qin, C.; Yang, B.; Melvin, T.M.; Fan, Z.; Zhao, Y.; Briffa, K.R. Radial growth of qilian juniper on the northeast tibetan plateau and potential climate associations. *PLoS ONE* **2013**. [\[CrossRef\]](#)
29. Bhutiyani, M.R.; Kale, V.S.; Pawar, N.J. Long-term trends in maximum, minimum and mean annual air temperatures across the Northwestern Himalaya during the twentieth century. *Clim. Chang.* **2007**, *85*, 159–177. [\[CrossRef\]](#)
30. Cybis Elektronik CDendro and CooRecorder. Available online: <http://www.cybis.se/forfun/dendro/> (accessed on 1 August 2018).
31. Holmes, R.L. Computer-assisted quality control in tree-ring dating and measurement. *Tree Ring Bull.* **1983**. [\[CrossRef\]](#)
32. Bunn, A.G. Statistical and visual crossdating in R using the dplR library. *Dendrochronologia* **2010**, *28*, 251–258. [\[CrossRef\]](#)
33. Grissino-Mayer, H.D. Evaluating crossdating accuracy: A manual and tutorial for the computer program COFECHA. *Tree Ring Res.* **2001**, *57*, 205–221.

-
34. Wigley, T.M.L.; Briffa, K.L.; Jones, P.D. On the average value of correlated time series, with applications in dendroclimatology and hydrometeorology. *Am. Meteorol. Soc.* **1984**, *23*, 201–213. [[CrossRef](#)]
 35. Bunn, A.G. A dendrochronology program library in R (dplR). *Dendrochronologia* **2008**, *26*, 115–124. [[CrossRef](#)]
 36. R Core Team. *R: A Language and Environment for Statistical Computing*; R Foundation for Statistical Computing: Vienna, Austria, 2017; Available online: <http://www.R-project.org/> (accessed on 17 March 2021).
 37. Cook, E.R. A Time Series Analysis Approach to Tree Ring Standardization. Ph.D Thesis, University of Arizona, Tucson, Arizona, 1995.
 38. Malik, R.; Rossi, S.; Sukumar, R. Cambial phenology in *Abies pindrow* (Pinaceae) along an altitudinal gradient in northwestern Himalaya. *IAWA J.* **2020**, *41*, 186–201. [[CrossRef](#)]
 39. Malik, R.; Rossi, S.; Sukumar, R. Variations in the timing of different phenological stages of cambial activity in *Abies pindrow* (Royle) along an elevation gradient in the north-western Himalaya. *Dendrochronologia* **2020**, *59*, 125660. [[CrossRef](#)]
 40. Fritts, H.C.C.; Guiot, J.; Gordon, G.A.A.; Schweingruber, F. Methods of Calibration, Verification, and Reconstruction. In *Methods of Dendrochronology*; Springer: Dordrecht, The Netherlands, 1990; pp. 163–217.
 41. Torrence, C.; Compo, G.P. A Practical Guide to Wavelet Analysis. *Bull. Am. Meteorol. Soc.* **1998**, *79*, 61–78. [[CrossRef](#)]
 42. Takahashi, K.; Azuma, H.; Yasue, K. Effects of climate on the radial growth of tree species in the upper and lower distribution limits of an altitudinal ecotone on Mount Norikura, central Japan. *Ecol. Res.* **2003**, *18*, 549–558. [[CrossRef](#)]
 43. Schweingruber, F.H. *Tree Rings and Environment Dendrochronology*; Paul Haupt AG, Bern: Bern, Switzerland, 1996.
 44. Zhang, Q.-B.; Hebda, R.J. Variation in radial growth patterns of *Pseudotsuga menziesii* on the central coast of British Columbia, Canada. *Can. J. For. Res.* **2004**, *34*, 1946–1954. [[CrossRef](#)]
 45. Fan, Z.-X.; Bräuning, A.; Cao, K.-F.; Zhu, S.-D. Growth–climate responses of high-elevation conifers in the central Hengduan Mountains, southwestern China. *For. Ecol. Manag.* **2009**, *258*, 306–313. [[CrossRef](#)]
 46. Dang, H.; Zhang, Y.; Zhang, K.; Jiang, M.; Zhang, Q. Climate-growth relationships of subalpine fir (*Abies fargesii*) across the altitudinal range in the Shennongjia Mountains, central China. *Clim. Chang.* **2013**, *117*, 903–917. [[CrossRef](#)]